

Simultaneous Step-size and Path Control for Efficient Transient Noise Analysis

Werner Römisch, Thorsten Sickenberger, and Renate Winkler

Abstract Noise in electronic components is a random phenomenon that can adversely affect the desired operation of a circuit. Transient noise analysis is designed to consider noise effects in circuit simulation. Taking noise into account by means of Gaussian white noise currents, mathematical modelling leads to stochastic differential algebraic equations (SDAEs) with a large number of small noise sources. Their simulation requires an efficient numerical time integration by mean-square convergent numerical methods. As efficient approaches for their integration we discuss adaptive linear multi-step methods, together with a new step-size and path selection control strategy. Numerical experiments on industrial real-life applications illustrate the theoretical findings.

1 Transient noise analysis in circuit simulation

In current chip design the decreasing feature sizes, high clock frequencies and low supply voltages cause several parasitic effect. As a consequence the signal-to-noise ratio decreases, i.e., the difference between the desired signal and noise is getting smaller. To address the signal-to-noise ratio the modelling and the simulation can be improved by taking the inner electrical noise into account. An important requirement for a transient noise simulation is the appropriate modelling of the noise

Werner Römisch

Inst. of Mathematics, Humboldt-Universität zu Berlin, 10099 Berlin, Germany,
e-mail: romisch@math.hu-berlin.de

Thorsten Sickenberger (Corresponding author)

Dept. of Mathematics, Heriot-Watt University, Edinburgh EH14 4AS, United Kingdom,
e-mail: t.sickenberger@hw.ac.uk

Renate Winkler

Dept. of Mathematics, Bergische Universität Wuppertal, 42199 Wuppertal, Germany,
e-mail: winkler@math.uni-wuppertal.de

sources in the time domain. We consider two different sources of inner electrical noise, namely, thermal noise of resistors and shot noise of semiconductors. Thermal noise i_{th} of resistors is caused by the thermal motion of electrons and is described by Nyquist's theorem. Shot noise i_{shot} of pn -junctions, caused by the discrete nature of currents due to the elementary charge, is modelled by Schottky's formula and inherits noise intensities that depend on the deterministic currents (see e.g. [1, 2]).

A noisy element is modelled as an additional stochastic current source in parallel to the original electronic element. The noise intensity is given by the physical characteristics and the noise models are added to the network equations. Combining Kirchhoff's current law with the element characteristics and using the charge-oriented formulation formally yields a stochastic differential-algebraic equation (SDAE) of the type (see e.g. [3, 4])

$$A \frac{d}{dt} q(x(t)) + f(x(t), t) + \sum_{r=1}^m g_r(x(t), t) \xi_r(t) = 0, \quad (1)$$

where A is a constant singular incidence matrix determined by the topology of the dynamic circuit parts, the vector $q(x)$ consists of the charges and the fluxes, and x is the vector of unknowns consisting of the nodal potentials and the branch currents through voltage-defining elements. The term $f(x, t)$ describes the impact of the static elements, $g_r(x, t)$ denotes the vector of noise intensities (amplitudes) for the r -th noise source, and $\xi := (\xi_1, \dots, \xi_m)^T$ is an m -dimensional vector of independent Gaussian white noise sources (see e.g. [1]).

Although this system (1) appears to be similar to a noise-free system, it requires a completely different mathematical background. A serious mathematical description begins by introducing the Brownian motion or the Wiener process that is caused by integrating the white noise " $W(t) = \int_0^t \xi(s) ds = \int_0^t dW(s)$ " (see e.g. [5]). Problem (1) is then understood as a stochastic integral equation

$$Aq(X(s)) \Big|_{t_0}^t + \int_{t_0}^t f(X(s), s) ds + \sum_{r=1}^m \int_{t_0}^t g_r(X(s), s) dW_r(s) = 0, \quad t \in [t_0, T], \quad (2)$$

where the second integral is an Itô-integral, and W denotes an m -dimensional Wiener process (or Brownian motion) given on the probability space (Ω, \mathcal{F}, P) with a filtration $(\mathcal{F}_t)_{t \geq t_0}$. The solution is a stochastic process depending on the time t and on the random sample ω where the argument ω is usually dropped. The value at fixed time t is a random variable $X(t, \cdot) = X(t)$ - for a fixed realization of the driving Wiener process, the function $X(\cdot, \omega)$ is called a path of the solution. Due to the influence of the Gaussian white noise, typical paths of the solution are rough and nowhere differentiable.

In current chip design one has to deal with a large number of equations as well as of noise sources. Fortunately, the noise intensities are small compared to the other quantities which can be used for the construction of efficient numerical schemes.

The focus here is on efficient numerical methods to simulate sample solution paths, i.e., strong approximations of the solution of the arising large systems of

SDAEs, since only such paths can reveal the phase noise. The calculation of hundreds or even a thousand solution paths are necessary for getting sufficient numerical confidence about the phase. Moreover, from the solution paths any other statistical data and measurements can be computed in a postprocessing step.

In this paper we present variable step-size two-step methods, in particular stochastic analogues of the trapezoidal rule and the two-step backward differentiation formula, see Section 2. The applied step-size control strategy is described in Section 3. Here we extensively use the smallness of the noise. In Section 4 new ideas for the control both of time and chance discretization are discussed. Test results that illustrate the performance of the presented methods are given in Section 5.

2 Adaptive numerical methods

The key idea to design methods for SDAEs is to force the iterates to fulfill the constraints of the SDAE at the current time-point. We consider stochastic analogues of methods that have proven very useful in the deterministic circuit simulation. Paying attention to the DAE structure, the discretization of the deterministic part (drift) is implicit, whereas the discretization of the stochastic part (diffusion) is explicit.

We consider stochastic analogues of the variable coefficient two-step backward differentiation formula (BDF₂) and the trapezoidal rule, where only the increments of the driving Wiener process are used to discretize the diffusion part. Analogously to the Euler-Maruyama scheme we call such methods multi-step Maruyama methods. The variable step-size BDF₂ Maruyama method for the SDAE (2) has the form (see [6] and, for constant step-sizes, e.g. [7])

$$A \frac{\alpha_{0,\ell} q(X_\ell) + \alpha_{1,\ell} q(X_{\ell-1}) + \alpha_{2,\ell} q(X_{\ell-2})}{h_\ell} + \beta_{0,\ell} f(X_\ell, t_\ell) + \alpha_{0,\ell} \sum_{r=1}^m g_r(X_{\ell-1}, t_{\ell-1}) \frac{\Delta W_r^\ell}{h_\ell} - \alpha_{2,\ell} \sum_{r=1}^m g_r(X_{\ell-2}, t_{\ell-2}) \frac{\Delta W_r^{\ell-1}}{h_\ell} = 0, \quad (3)$$

$\ell = 2, \dots, N$. Here, X_ℓ denotes the approximation to $X(t_\ell)$, $h_\ell = t_\ell - t_{\ell-1}$, and $\Delta W_r^\ell = W_r(t_\ell) - W_r(t_{\ell-1}) \sim N(0, h_\ell)$ on the grid $0 = t_0 < t_1 < \dots < t_N = T$. The coefficients $\alpha_{0,\ell}, \alpha_{1,\ell}, \alpha_{2,\ell}, \beta_{0,\ell}$ depend on the step-size ratio $\kappa_\ell = h_\ell/h_{\ell-1}$ and satisfy the conditions for consistency of order one and two in the deterministic case. Let the coefficients of the scheme be normalized in such a way that $\alpha_{0,\ell} = 1$ for all ℓ .

A correct formulation of the stochastic trapezoidal rule for SDAEs requires more structural information (see [8]). It should implicitly realize the stochastic trapezoidal rule for the so called inherent regular SDE of (2) that governs the dynamical components. Both the BDF₂ Maruyama method and the stochastic trapezoidal rule of Maruyama type have only an asymptotic order of strong convergence of 1/2, i.e.,

$$\|X(t_\ell) - X_\ell\|_{L_2(\Omega)} := \max_{\ell=1, \dots, N} (E|X(t_\ell) - X_\ell|^2)^{1/2} \leq c \cdot h^{1/2}, \quad (4)$$

where $h := \max_{\ell=1, \dots, N} h_\ell$ is the maximal step-size of the grid. This holds true for all numerical schemes that include only information on the increments of the Wiener process. However, the noise densities given in Section 1 contain small parameters and the error behaviour is much better. In fact, the errors are dominated by the deterministic terms as long as the step-size is large enough [6, 7].

In more detail, the error of the given methods behaves like $O(h^2 + \varepsilon h + \varepsilon^2 h^{1/2})$, when ε is used to measure the smallness of the noise, i.e., $g_r(x, t) = \varepsilon \hat{g}_r(x, t)$, $r = 1, \dots, m$ where $\varepsilon \ll 1$. Thus we can expect order 2 behaviour if $h \gg \varepsilon$. Higher numerical effort for higher deterministic order pays off only if the noise is *very* small.

3 Local error estimates

The smallness of the noise allows us to construct special estimates of the local error terms, which can be used to control the step-size. We aim at an efficient estimate of the mean-square of dominating local errors by means of a sufficiently large number of simultaneously computed solution paths. This leads to an adaptive step-size sequence that is identical for all paths. For the drift-implicit Euler-Maruyama scheme this step-size control has been presented in [9], see also [1, 4].

In [8, 10] the authors extended this strategy to stochastic linear multi-step methods with deterministic order 2 and provided a reliable error estimate. Let \tilde{L}_ℓ approximate the dominating local error in $Aq(X_\ell)$ by

$$\tilde{L}_\ell = c_\ell h_\ell \frac{2\kappa_\ell}{\kappa_\ell + 1} \left[f(X_\ell, t_\ell) - (\kappa_\ell + 1)f(X_{\ell-1}, t_{\ell-1}) + \kappa_\ell f(X_{\ell-2}, t_{\ell-2}) \right], \quad (5)$$

where c_ℓ is the error constant of the related deterministic scheme and κ_ℓ is the step-size ratio. The estimate (5) is based on already computed values of the drift term. Recall that \tilde{L}_ℓ is a vector valued random variable as is the solution X_ℓ . In dependence on the small parameter ε and the step-size h_ℓ the L_2 -norm of the local error behaves like $O(h_\ell^3 + \varepsilon h_\ell^{3/2} + \varepsilon^2 h_\ell)$. The term of order $O(h_\ell^3)$ dominates the local error behaviour as long as h_ℓ^3 is much larger than $\varepsilon h_\ell^{3/2}$, i.e., $\varepsilon^{2/3} \ll h_\ell$. Under this condition also the expression $\|\tilde{L}_\ell\|_{L_2}$ approximates the local error at time t_ℓ .

Depending on the available information we will monitor different quantities to satisfy accuracy requirements,

- I. control $\|(A + h_\ell \beta_{0,\ell} J_\ell)^{-1} \tilde{L}_\ell\|_{L_2}$ to match a given tolerance for X_ℓ ,
- II. control $\|\tilde{L}_\ell\|_{L_2}$ to match a given tolerance for $Aq(X_\ell)$, or
- III. control $\|A^- \tilde{L}_\ell\|_{L_2}$ to match a given tolerance for $Pq(X_\ell)$.

Here J is the Jacobian of the drift function f w.r.t. the first variable, and A^- denotes the pseudo inverse of A with $A^- A = P$, where P is a projector onto the dynamic components of $q(X_\ell)$ [11]. Since $(A/h_\ell + \beta_{0,\ell} J_\ell) = 1/h_\ell \cdot (A + h_\ell \beta_{0,\ell} J_\ell)$ is the Jacobian of the discrete scheme (3) this matrix (or a good approximation to it) and its

factorization are usually available. In case of M sampled paths, the L_2 -norm in (I)–(III) is approximated by using the M values J_ℓ^i and \tilde{L}_ℓ^i ($i = 1, \dots, M$) that use values X_ℓ^i , $X_{\ell-1}^i$, and $X_{\ell-2}^i$ from the i th path. For example, in case (I) we use

$$\left\| (A + h_\ell \beta_{0,\ell} J_\ell)^{-1} \tilde{L}_\ell \right\|_{L_2} \approx \left(\frac{1}{M} \sum_{i=1}^M \left| (A + h_\ell \beta_{0,\ell} J_\ell^i)^{-1} \tilde{L}_\ell^i \right|^2 \right)^{1/2} =: \hat{\eta}_\ell. \quad (6)$$

Especially in circuit simulation the different ways of scaling the defect will enable us to control different quantities of the solution. In (I) the local error estimate is used unscaled to match a given tolerance based on a vector representing the charges and the fluxes of the electronic network. Considering the second case (II), the scaled error estimate can be used to match a given tolerance for the solution $X_\ell = (e, j_L, j_V)$ which represent the nodal potentials and some branch currents.

4 A solution path tree algorithm

In the analysis so far, we have considered a constant number M of sample paths. These number influences the approximation of the solution as well as of the mean-square norm in (6). There we make an additional error, the so-called sampling error ϑ_ℓ , and the error expansions reads $\|\tilde{L}_\ell\|_{L_2} = \hat{\eta}_\ell + \vartheta_\ell$, where $\hat{\eta}_\ell$ is the approximation of the dominating local error term based on the sample paths. The idea is to control also the number of sample paths using an estimate of ϑ_ℓ . This yields an approximate solution which consists of a tree of paths that is extended, reduced or kept fixed adaptively.

Our aim in tuning the number of paths is to balance the local error and the sampling error. Let STOL_ℓ be the tolerance for the sampling error ϑ_ℓ at time t_ℓ . One possibility is to calculate this tolerance as an approximation of the higher deterministic error term of order $O(h_\ell^4)$. We then derive the best number M_ℓ of paths

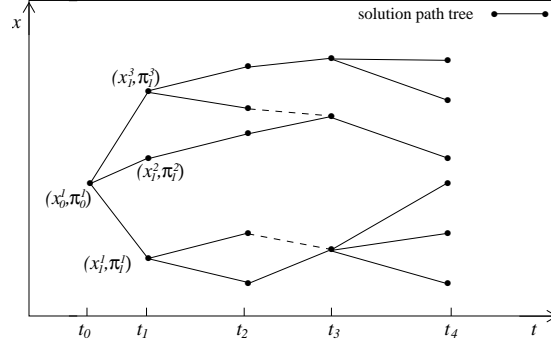


Fig. 1 A solution path tree: Variable time-points t_ℓ , solution states x_ℓ^j and path weights π_ℓ^i .

by

$$M_\ell = \left\lceil \frac{1}{\text{STOL}_\ell^2} \frac{\hat{\mu}_\ell^2 \cdot \hat{\sigma}_\ell^2}{\hat{\mu}_\ell^2 + \hat{\sigma}_\ell^2} \right\rceil, \quad (7)$$

(see [4]), where $\hat{\mu}_\ell$ and $\hat{\sigma}_\ell^2$ are estimates of the mean and the standard deviation of the error estimate at time-point t_ℓ , respectively. Here $\lceil x \rceil$ denotes the smallest integer greater or equal to x .

The best number of paths M_ℓ depends on the time-point t_ℓ and is realized by approximate solutions generated on a tree of paths that is extended, reduced or kept fixed adaptively. In [4, 12] the authors describe the construction of a solution path tree in detail. The method uses probabilities π_ℓ^i ($\ell = 1, \dots, N; i = 1, \dots, M_\ell$) to weight the solution paths. Figure 1 gives an impression, how a solution path tree looks like. Here the dashed lines indicates the optimal redistribution of the weights after a reduction step (see [4] for a detailed description of the path tree generation).

At each time-step the optimal expansion or reduction problem is formulated by means of combinatorial optimization models. The path selection is modelled as a mass transportation problem in terms of the L_2 -Wasserstein metric (see [13] in context of scenario reduction in stochastic programming). The algorithm has been implemented in practice. The results presented in the next section show its performance.

5 Numerical results

Here we present numerical experiments for the stochastic BDF₂ applied to a test circuit examples. To be able to handle real-life problems, a slightly modified version of the schemes has been implemented in Qimonda's in-house analog circuit simulator TITAN. We consider a model of an inverter circuit with a MOSFET transistor, under the influence of thermal noise. The related circuit diagram is given in Figure 2. The MOSFET is modelled as a current source from source to drain that is controlled by the nodal potentials at gate, source and drain. The thermal noise of the resistor and of the MOSFET is modelled by additional white noise current sources that are shunt

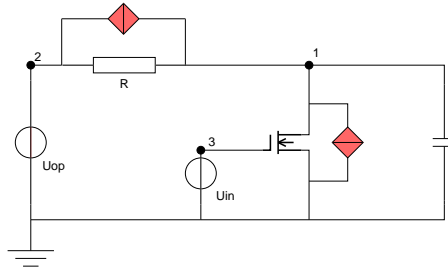


Fig. 2 Thermal noise current sources in a MOSFET inverter circuit marked by grey diamonds.

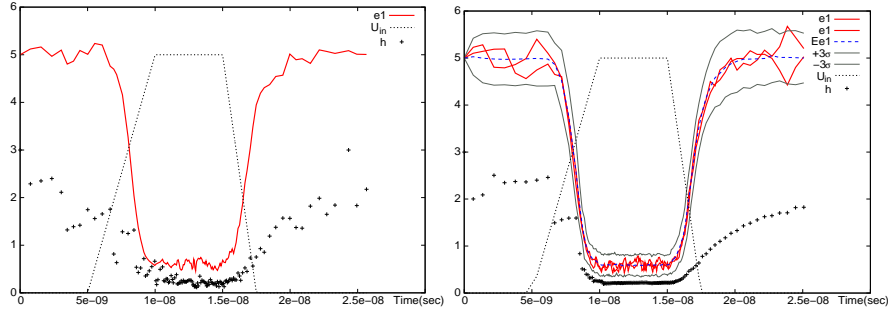


Fig. 3 Simulation results for the noisy inverter circuit:

Left: 1 path, 127 (+29 rejected) steps;

Right: 100 paths, 134 (+11 rejected) steps.

in parallel to the original, noise-free elements. To highlight the effect of the noise, we scaled the diffusion coefficient by a factor of 1000.

In Figure 3 we present simulation results, where we plotted the input voltage U_{in} and values of the output voltage e_1 versus time. Moreover, the applied step-sizes, suitably scaled, are shown by means of single crosses. We compare the results for the computation of a single path (left) with those for the computation of 100 simultaneously computed solution paths (right). The additional solid lines show two arbitrarily chosen solution paths, the dashed line gives the mean of 100 paths and the outer thin lines the 3σ -confidence interval (computed as a statistical estimate for the standard deviation) for the output voltage e_1 . We observe that using the information of an ensemble of simultaneously computed solution paths smoothes the step-size sequence and considerably reduces the number of rejected steps, when compared to the simulation of a single path. The computational cost that is mainly determined by the number of computed (accepted + rejected) steps is reduced.

Additionally we have applied the solution path tree algorithm to this example. The upper graph in Figure 4 shows the computed solution path tree together with the applied step-sizes which are used simultaneously for all path segments. The lower graph shows the simulation error (solid line), its tolerance (dashed line) and the used number of paths (marked by \times), vs. time. Here the tolerance is determined by an approximation of the deterministic local error of order $O(h^4)$ (see [10]) and the maximal number of paths was set to 250. The results indicate that there exists a region from nearly $t = 1 \cdot 10^{-8}$ up to $t = 1.5 \cdot 10^{-8}$ where we have to use much more than 100 paths. This is exactly the area in which the MOSFET is active and the input signal is inverted. Outside this region the algorithm proposes approximately 70 simultaneously computed solution paths.

Especially in circuit simulation the solution path tree algorithm provides an advantage. It helps the designer to identify critical noisy elements of the circuit. In this example the active MOSFET featuring nonlinear noise causes a high fluctuation in the local error estimate whereas the additive noise of the linear resistor behaves harmless.

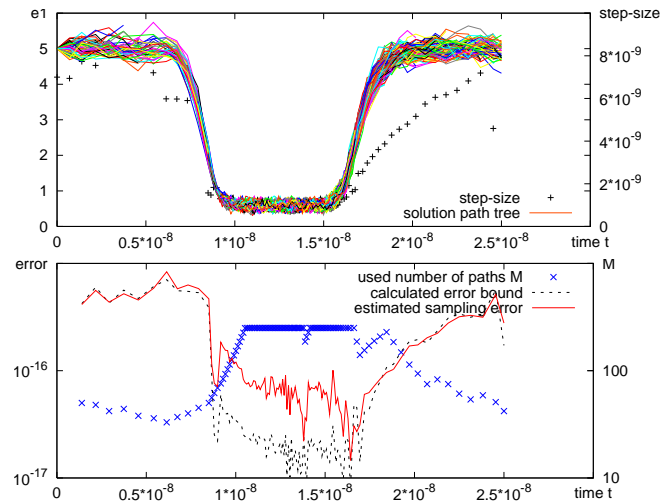


Fig. 4 Simulation results for the noisy inverter circuit: Solution path tree and step-sizes (top), sampling error, its error bound and the number of paths (bottom).

References

1. Denk, G., Winkler, R.: Modeling and simulation of transient noise in circuit simulation. *Math. and Comp. Modelling of Dyn. Systems*, **13**(4), 383–394 (2007)
2. Sickenberger, T., Winkler, R.: Adaptive Methods for Transient Noise Analysis. In: G. Ciuprina, D. Ioan (eds.) *Scientific Computing in Electrical Engineering SCEE 2006, Mathematics in Industry*, vol. 11, pp. 161–166. Springer, Berlin (2007)
3. Winkler, R.: Stochastic differential algebraic equations of index 1 and applications in circuit simulation. *J. Comput. Appl. Math.*, **157**(2), 477–505 (2003)
4. Sickenberger, T.: Efficient Transient Noise Analysis in Circuit Simulation. Ph.D. thesis Humboldt Universität zu Berlin, Logos Verlag, Berlin (2008)
5. Arnold, L.: *Stochastic differential equations: Theory and Applications*. Wiley, New York (1974)
6. Sickenberger, T.: Mean-square convergence of stochastic multi-step methods with variable step-size. *J. Comput. Appl. Math.*, **212**(2), 300–319 (2008)
7. Buckwar, E., Winkler, R.: Multi-step methods for SDEs and their application to problems with small noise. *SIAM J. Num. Anal.*, **44**(2), 779–803 (2006)
8. Sickenberger, T., Weinmüller, E., Winkler, R.: Local error estimates for moderately smooth problems: Part II – SDEs and SDAEs. To appear in *BIT Numerical Mathematics*
9. Römisch, W., Winkler, R.: Stepsize control for mean-square numerical methods for SDEs with small noise. *SIAM J. Sci. Comp.*, **28**(2), 604–625 (2006)
10. Sickenberger, T., Weinmüller, E., Winkler, R.: Local error estimates for moderately smooth problems: Part I – ODEs and DAEs. *BIT Numerical Mathematics*, **47**(2), 157–187 (2007)
11. Estévez Schwarz, D., Tischendorf, C.: Structural analysis of electric circuits and consequences for MNA. *Int. J. Circ. Theor. Appl.*, **28**, 131–162 (2000)
12. Römisch, W., Sickenberger, Th.: On generating a solution path tree for efficient step-size control. In preparation.
13. Dupačová J., Gröwe-Kuska, N., Römisch, W.: Scenario reduction in stochastic programming. *Math. Program., Ser. A* **95**, 493–511 (2003)
14. Higham, D.J.: An algorithmic introduction to numerical simulation of stochastic differential equations. *SIAM Review*, **43**, 525–546 (2001)